Efficiency Improvements in a Servoless Swash Plate Pump: Experimental and Simulation Results

Nathaniel J. Fulbright[1]*, Samuel Hall[2], Matthew Creswick[3], Stanislav Smolka[4], Robert Rahmfeld[5]

[1]*Danfoss Power Solutions, Hydrostatics Engineering, 14615 Lone Oak Rd, Eden Prairie, MN, 55344, USA*
[2]*Danfoss Power Solutions, Research and Development, Centers of Excellence, 2800 E 13th St, Ames, IA, 50010, USA*
[3]*Danfoss Power Solutions, Open Circuit Pumps Engineering, 14615 Lone Oak Rd, Eden Prairie, MN, 55344, USA*
[4]*Danfoss Power Solutions, Hydrostatics Engineering, 2800 E 13th St, Ames, IA, 50010, USA*
[5]*Danfoss Power Solutions, Hydrostatics Engineering, Krokamp 35, 24539 Neumünster, Germany*

*Corresponding author. Email: nate.fulbright@danfoss.com

Abstract

Variable displacement axial piston units conventionally use a servo system (consisting of a servo piston and valve) to adjust and control their displacement. In a novel design approach, the traditional servo system is removed, and the displacement is adjusted only by the loads on the swash plate. By employing specialized valve plate porting and control logic, the design allows for the displacement to be controlled without a servo system, improving efficiency and reducing complexity and size, and also introduces the ability to adjust the cross-port area profile of the valve plate. This adaptability significantly reduces cross-port flow and its associated losses, particularly in low-flow, high-pressure conditions, and it enables tunability in efficiency and noise. Previous work has demonstrated the controllability of a servoless swash plate pump. In this work, theorized efficiency improvements are confirmed by experimental data indicating up to an 18% improvement in overall pump efficiency. A 1D simulation modeling approach is presented, detailing the unique considerations that must be considered for a servoless pump. The simulation model produces efficiency improvement predictions that are generally within ±3% of the experimental results and are often within ±2%.

1 INTRODUCTION

Swash plate type axial piston units are ubiquitous in industrial and mobile fluid power systems due to their high efficiency, robustness, and high power-density. While fixed displacement swash plate units are used in many applications, variable displacement units offer enhanced flexibility to support a wide range of operating conditions. Conventionally, variable displacement units use a hydraulic servo piston that must overcome all internal forces that act to change the displacement of the unit[1]. As the internal forces increase, either the size of the servo piston must increase (increasing the package size of the unit) or the servo piston must run at higher pressures (leading to increased power consumption). Additionally, mechanical feedback methods used in variable displacement units, like the complex feedback linkage found in many swash plate pumps, further complicates the design. Despite these challenges, servo pistons persist as the *de facto* choice due to limited availability of alternative solutions capable of effectively controlling the immense and varying internal forces applied to the swash plate. However, a shift in perspective to view the internal forces as a potential asset rather than something to overcome allows more solutions to emerge.

One potential solution is to completely remove the servo piston and use the loads on the swash plate to control the stroke of the unit. Removing the servo piston leads to a smaller package, reduced hardware complexity, and a complete removal of servo system losses, but it also yields tangible performance enhancements. Several patents present designs that remove the servo piston [1,2,3], but available scientific research is limited. Cho presented a servoless pump that utilized valve plate indexing to vary the moments on the swash plate [4]. That work focused on developing control methodologies using a reduced order model, but it did not examine the effects of the control strategy on efficiency. Furthermore, the design deviates from a traditional swash plate pump design by introducing a valve plate that rotates to change the indexing.

The most promising approach to achieving a servoless pump was introduced by Tvarůžek with the concept of a "dynamic valve plate" [5]. By adding additional ports feeding into control valves at each dead center position, the cross-port area profile can be dynamically adjusted throughout the operating range of the unit. In contrast to a

[1] Direct displacement control is another approach to enabling variable displacement in swash plate units, but this paper only focuses on units with a servo system.

conventional “static” valve plate, the dynamic valve plate enables tunable efficiency and noise levels and the ability to change the operating characteristics (e.g., switch between high-efficiency and low-noise modes). Furthermore, the variable cross-porting can greatly reduce cross-port flow and associated losses, especially at low-flow high-pressure operating conditions. This design requires only minimal modifications to existing production pump hardware, although it does introduce the requirement for a microcontroller to select the appropriate control valve opening for a given operating condition. The fluid power industry is looking for more efficient technologies but cannot easily support drastic changes in architecture [6], so the dynamic valve plate approach is well aligned with industry desires.

The proof-of-concept design presented in [5] demonstrated controllability of a servoless swash plate pump using only forces generated by the rotating kit. While these initial achievements demonstrate the feasibility and benefits of displacement control without a servo piston, further considerations are needed for a production-ready unit. Efficiency, noise, stability, and dynamic response to commands must be well-understood and optimized. To expedite this design work and guide control-logic optimization, simulation is the ideal tool.

In this work, the efficiency improvements of a servoless pump are demonstrated. The operating principles of the dynamic valve plate that enable the servoless pump displacement control are summarized, and the 1D modeling approach that is required for a servoless pump is discussed. Experimental results are presented and used to determine the accuracy of the simulation model.

2 Dynamic Valve Plate and Servoless Unit Operating Principles

Note: For a detailed explanation of the dynamic valve plate and servoless unit operating principles, refer to [5].

The servoless swash plate unit concept eliminates the servo piston and uses the moments applied to the swash plate by the rotating kit to control the position of the swash plate. This is accomplished by manipulating the piston chamber pressure during the transition between the high- and low-pressure ports. Pressure during the transition between ports is regulated via a control port connected to a variable valve, collectively referred to as the dynamic valve plate (Figure 1). The effect of the control valve is the same as that of conventional porting features on a static valve plate: connect the piston chamber to the oncoming pressure port. For a given operating condition, the valve opening is constant and does not change during individual piston transitions.

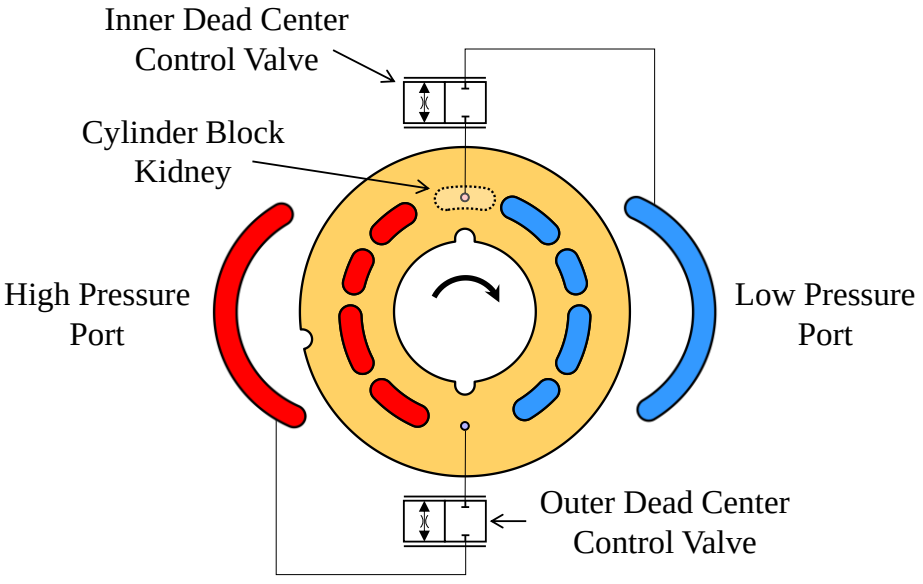

Figure 1 Dynamic Valve Plate Showing Valve Connections to Transitions [2]

The behavior of the piston chamber pressure profile during the transition is primarily influenced by the interaction between the control valve opening and the compressibility of the fluid. Throughout the pressure transition, the volume of the piston chamber remains relatively constant. At inner dead center (IDC), the piston chamber transitions from high to low pressure, while at outer dead center (ODC), it transitions from low to high pressure. When the control valves are open (as depicted in the top panel of Figure 2), the IDC piston maintains low pressure during

the transition and the ODC piston maintains high pressure. The larger the control valve opening, the faster the piston chamber pressures transition. The net effect of the pressure forces on the swash plate causes the swash plate angle to increase, causing on-stroking behavior. Conversely, when the control valves are closed (as shown in the bottom panel of Figure 2), the IDC piston prematurely rises to high pressure and the ODC piston prematurely drops to low pressure, de-stroking the pump. Leakage and the small changes in the piston chamber volume during the transition also impact the pressure profiles, though to a lesser degree. Achieving stable displacement under specific operating conditions involves commanding the valves to appropriate openings that balance all piston forces on the swash plate (including pressure, friction, and inertia) with other external moments, such as those from springs.

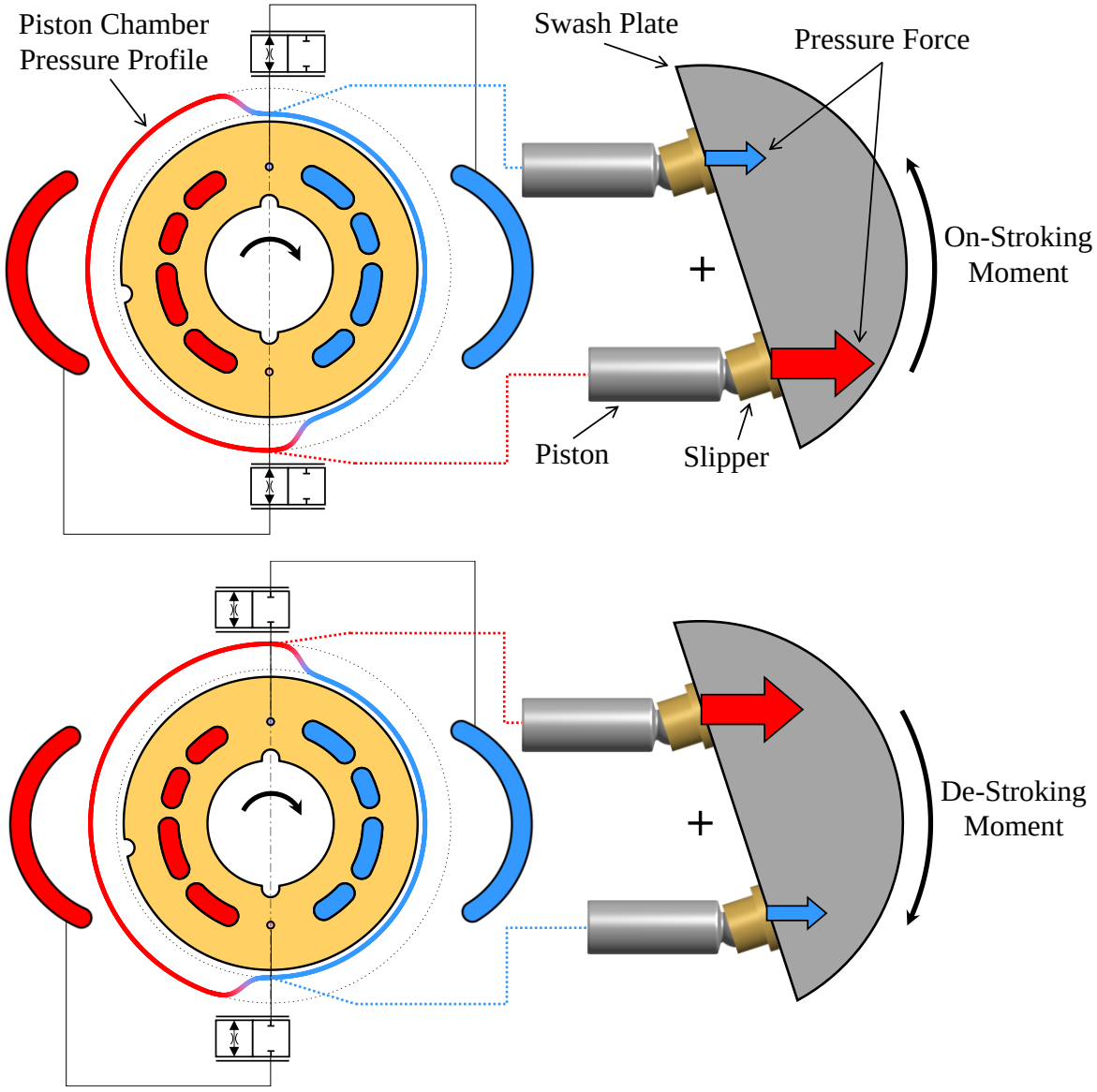

Figure 2 Pressure Transition Variation with IDC and ODC Valves Open (Top) and Closed (Bottom)

When the control valves are closed, there is little to no cross-port flow, resulting in reduced loss compared to conventional pump valve plates. Conventional pump valve plates often incorporate cross-porting for noise reduction, prevention of cavitation, or modification of the swash plate moments. As the control valves open, cross-port flow increases, leading to increased loss. The efficiency improvement in a servoless pump primarily stems from the decreased cross-port flow.

3 SIMULATION MODEL

In a conventional swash plate unit with a servo piston, the rotating kit can be simulated and analyzed relatively independently from the servo system. This allows for models with lower complexity while maintaining fidelity for the relevant metrics such as efficiency and pressure ripple for the rotating kit and step-response and stability for the servo system. For a servoless unit, the rotating kit *is* the servo system, requiring the single model to contain additional dynamic degrees of freedom for the displacement adjustment. For example, instead of predefining the motion of the swash plate, the swash plate motion is calculated given the forces applied to it. Mechanical and hydraulic losses, typically only used for efficiency predictions and treated as noise to be rejected by the servo system, now play an important role in determining the control behavior of the unit.

Many modeling approaches exist, ranging from simple equations for theoretical flow rate to complex 3D multiphysics modeling. A useful middle ground between these two extremes is 1D modeling, which provides significant insight into the dynamics of the system while being substantially less computationally expensive than 3D multiphysics modeling.

3.1 Fundamental Modeling Techniques

Each piston chamber is considered its own control volume with multiple fluid flow paths to and from the volume. Flow between the piston chamber and the end cap passes through the valve plate, which is modeled as an orifice with a constant or flow-dependent discharge coefficient. Additional flow between the piston chamber and the pump case occurs due to leakage between the piston and the bore, the slipper and the swash plate, the cylinder block and valve plate, and the valve plate and the end cap. The volumes of the piston chambers and the kinematics of the pistons are calculated as a function of the pump geometry, shaft motion (position, velocity, and acceleration), and swash plate motion (position, velocity, and acceleration). These kinematic calculations are closed form and are formulated to allow for time-varying swash plate motion. The instantaneous pressure (p) within each piston chamber is calculated by solving the pressure build-up differential equation shown in Equation (1), which accounts for fluid stiffness (β), piston chamber volume (V), and the net flow into or out of the piston chamber ($q_{V,net}$):

$$\frac{dp}{dt} = \frac{\beta}{V}\left(q_{v,net} - \frac{dV}{dt}\right) \tag{1}$$

The various flow rates for the next time step of the model are calculated using this new instantaneous piston chamber pressure, and the process iterates. Some simulation models do not model any more physics beyond those that have already been mentioned, especially those that are only concerned with pump hydraulic performance. However, the fluid-related aspects of the model are only the first aspect needed to accurately model a servoless swash plate pump.

The internal forces and moments of a swash plate pump provide the next level of information to analyze a servoless swash plate pump. The most basic approach is to include the pressure force on the pistons and the inertial forces of the piston-slipper assemblies. For some conventional pump models, this is sufficient for tasks like sizing a servo piston because the remaining non-ideal behavior is considered a noise factor to be robust against. However, for a servoless pump, these noise factors (i.e., friction) can have a large impact on the resulting swash plate moments. Piston-bore friction and slipper-swash plate friction are both substantial sources of friction in a swash plate pump, and during portions of the cycle, their effects compound and increase the overall piston friction force. Given that the swash plate reacts all axial force applied to the piston including pressure, inertia, and friction, accurate swash plate moment predictions necessitate considering all axial forces. Frictional losses such as valve plate-cylinder block friction, bearing friction, and shaft seal friction are unnecessary for swash plate moment predictions, but these losses are still useful for making more accurate pump efficiency predictions.

At this point, many pump models are considered complete; the hydraulic and mechanical behavior of the pump is well understood, including losses, and useful performance predictions can be made. Simulated performance maps can be generated, partial efficiencies can be determined, and the servo piston can be sized to maintain control authority for any operating condition. However, such a model is only marginally useful for a servoless swash plate unit. The swash plate motion must still be prescribed and cannot react to changes in the swash plate moment, a fundamental requirement dictated by the principles of servoless pump operation.

3.2 Dynamic Swash Plate

Instead of the swash plate angle being defined before the simulation, it is calculated based on the net moment applied to the swash plate. This net moment of course consists of the forces from the pistons and can also include forces and moments from other elements like springs, or for a conventional pump, the servo piston. Frictional moments and hysteresis can also be incorporated into the swash plate dynamics calculation. The introduction of a dynamic swash plate to the model enables prediction of the dynamic response of the pump to changes in displacement commands, and it also improves the fidelity of the predictions at steady-state conditions.

To hold the swash plate at a given angle, the mean moment on the swash plate must be zero, but that does not mean the instantaneous swash plate moment will be equal to the mean moment. Even in the most ideal case (no losses, no fluid compressibility, ideal valve timing, etc.), the finite number of pistons in a swash plate pump guarantees that the moment on the swash plate will not be a constant value throughout a revolution. For an unconstrained swash plate, like that found in a servoless pump, this means the swash plate will have instantaneously unbalanced moments and will oscillate about a mean angle. This behavior is also observed in pumps with a servo piston because the servo piston and the associated fluid volumes are not infinitely stiff.

The potentially larger swash plate oscillations in a servoless unit affect the kinematics of the piston, especially at the dead center positions where the piston velocity due to shaft rotation is near zero and the piston velocity due to swash plate rotation is the greatest. With the additional consideration that the flow area near the dead center positions is at a minimum, even relatively small changes in swash plate angle can significantly affect the piston pressure, especially if those changes are fast enough to outpace valve plate and leakage flow. Pistons at the dead center positions have the largest moment arm on the swash plate, further amplifying the effect of the pressure changes. The IDC and ODC pistons are inversely affected (e.g., swash plate motion that increases the IDC piston pressure will decrease the ODC piston pressure), leading to an oscillatory feedback loop between the swash plate motion and the dead center piston pressures.

The effects of the swash plate oscillation combined with all other effects in the model result in a sufficiently detailed understanding of the net moment applied to the swash plate. With this information, a control valve opening map can be generated for different operating conditions, linking each condition to the corresponding valve opening and ensuring a mean swash plate moment of zero. To change displacement, the control valve opening is changed following the map, and the “macro-level” dynamic swash plate behavior of the model is observed. Traditional control metrics such as rise time, settling time, and overshoot can be calculated for this behavior. Finally, the control valve opening map can be used to develop control algorithms.

4 EXPERIMENTAL RESULTS

4.1 Hardware Modifications

The same prototype closed-circuit servoless swash plate pump used in [5] was used to gather steady-state pump performance data. The pump is a variable displacement 130 cc swash plate pump with EDC control, and was tested in its unmodified state to gather benchmark data. The following modifications were made to the pump to make it a servoless pump:

- Grooves were added in the end cap to drain the servo piston oil to case. All other supply passages of control flow were also blocked. With no control pressure applied to the servo piston, the servo piston assembly acts as a damper to the motion of the swash plate.
- Internal passages were added in the end cap to connect the control ports on the valve plate to the respective control valves and to connect the control valves to the respective pump ports.
- Two control spool valves driven by proportional solenoids were added. The control valves mount to the servoless pump end cap.

All rotating kit components remained identical between the tests. A representative image of a servoless pump is shown in Figure 3.

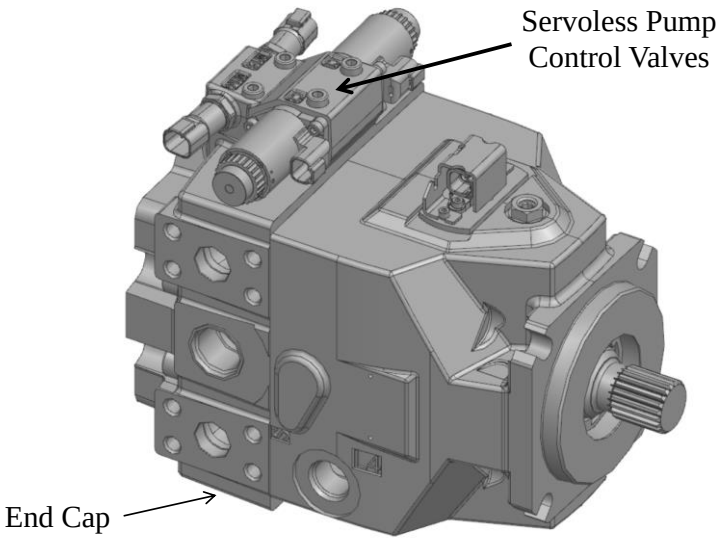

Figure 3 Servoless Pump

4.2 Operating Conditions and Data Collection

A total of four pressure and speed combinations were used to compare the servoless pump to the production pump in pumping mode: 100 and 200 bar pressure differentials and 1,000 and 2,000 RPM shaft speeds. For each combination, five swash plate angles (4, 8, 12, 16, and 18 degrees) were examined. The production pump used the EDC control to maintain the swash plate angle. The servoless pump used open-loop control of the control valves to hold the swash plate at the desired angle. Both control valves were opened the same amount for a given operating condition. For the servoless pump, effort was made to ensure minimal impact on the swash plate moments from the servo piston. No command was sent to the EDC control, the servo cans were drained to case, the servo gauge ports were connected to each other, and the control supply port was plugged – the servo piston and servo piston springs were only serving as a neutral return mechanism for the swash plate.

Testing was done in accordance with ISO 4409 using “class A” measurement accuracy [7]. All tests were done using Shell Tellus 46 S2 MX oil at 50 °C. The following measurements were recorded: swash plate angle, shaft angular velocity and torque, port pressures, outlet flow rate, and inlet fluid temperature. Sensors were sampled for 2 seconds at 2,000 Hz with an anti-aliasing filter applied and the readings were averaged. An external charge pump was used to supply 26 bar of charge pressure at 26 LPM (nominal).

4.3 Results

4.3.1 Servoless Pump Control Valve Solenoid Current

Figure 4 shows the current provided to the solenoids controlling the servoless pump control valves. The solenoid current trends upwards as swash plate angle increases. An increase in solenoid current corresponds to an increase in control valve opening area, although flow forces can also impact the current required to maintain a given valve opening area.

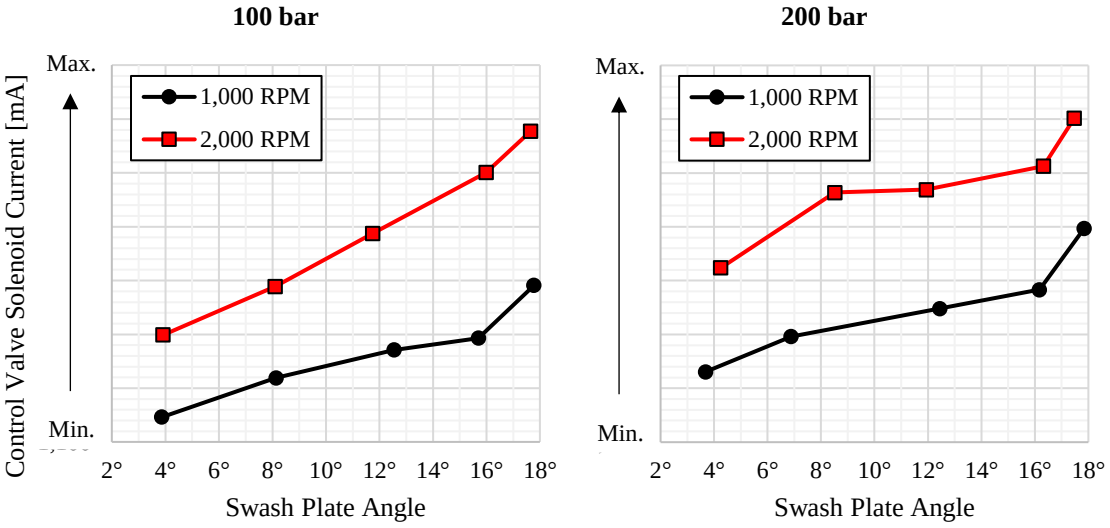

Figure 4 Servoless Pump Control Valve Solenoid Current

4.3.2 Overall Efficiency

Figure 5 shows the difference in overall efficiency between the servoless pump and the production pump. Overall efficiency, η_τ, is calculated as:

$$\eta_\tau = \frac{P_{out}}{P_{in}} \tag{2}$$

where P_{out} is the output power and P_{in} is the input power. Only the pump power is included in the efficiency calculations – power lost via the servo system and the power needed to drive the control valves are not included. For a pump, the output power is hydraulic power (Equation (3)) and the input power is mechanical power (Equation (4)):

$$P_{out} = \Delta p q_V \tag{3}$$

$$P_{in} = Tn \tag{4}$$

where Δp is the pressure differential between the primary ports of the pump, q_V is the volumetric flow rate at the outlet of the pump, T is the shaft torque, and n is the angular velocity of the shaft. The error bars in Figure 5 represent the uncertainty in the overall efficiency difference due to sensor accuracy compounding through the calculations.

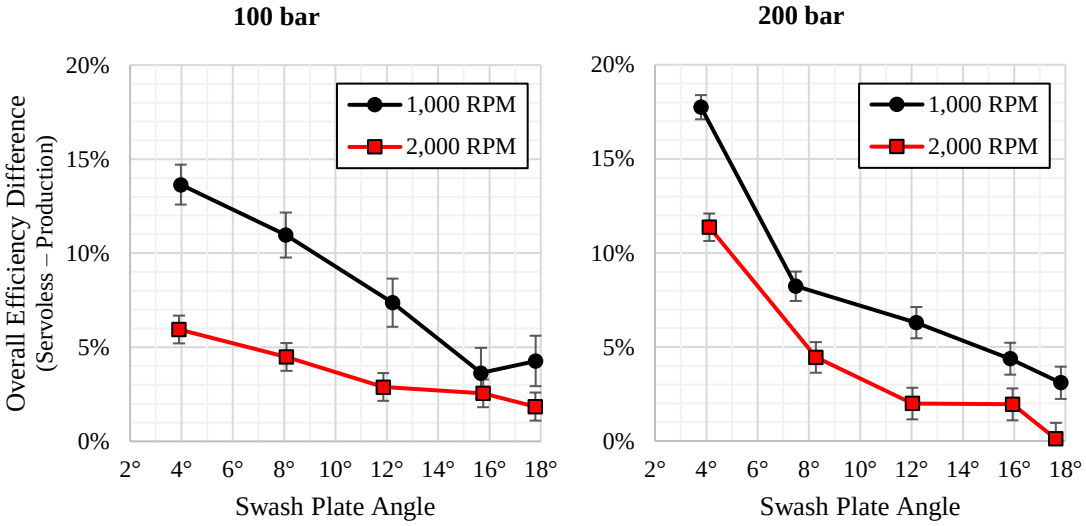

Figure 5 Overall Efficiency Difference Between Servoless Pump Prototype and Production Pump

Across all conditions, the servoless pump consistently outperforms the production pump, boasting a peak overall efficiency improvement of nearly 18%. This improvement in efficiency is more pronounced at lower shaft speeds and swash plate angles. The greatest efficiency improvements are at the minimum tested swash plate angle (4°) and highest pressure (200 bar) for both shaft speeds. However, as the swash plate angle increases, the efficiency difference for the high-pressure conditions becomes lower than the efficiency difference for the low-pressure conditions. Notably, the low-speed (1,000 RPM) results show a higher overall efficiency difference than the high-speed (2,000 RPM) results at all swash plate angles and pressure differentials.

4.3.3 Power Loss

Figure 6 shows the power loss reduction of the servoless pump relative to the production pump. Power loss, P_{loss}, is defined as:

$$P_{loss} = P_{in} - P_{out} \tag{5}$$

Just as with the overall efficiency, the servoless pump has reduced power loss relative to the production pump at all tested conditions. For most operating conditions, the power loss is at least 1 kW lower than the production pump, with a peak power loss reduction of over 2 kW. The power loss is roughly constant across the range of swash plate angles for the 100 bar data sets, showing a consistent power loss reduction of approximately 1 kW. Conversely, the power loss comparison for the 200 bar data sets is more varied, with both data sets beginning with a 2 kW power loss reduction at the lowest swash plate angle (4°), followed by diminishing power loss reductions as the swash plate angle increases. The data set at 1,000 RPM and 200 bar demonstrates a 1.5 kW power loss reduction at full stroke, while the data set at 2,000 RPM and 200 bar data set exhibits minimal change in power loss (relative to the production pump) at full stroke.

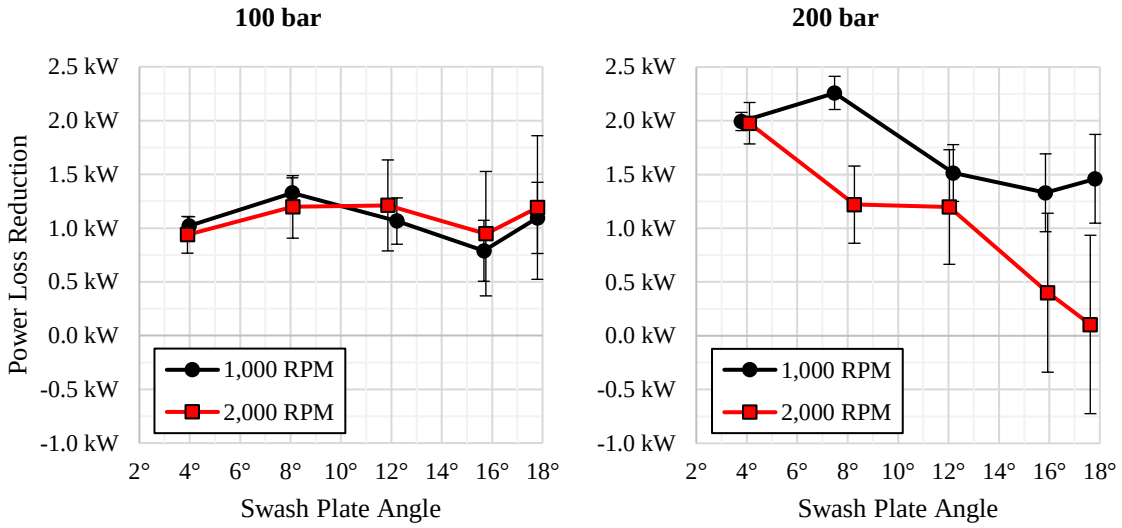

Figure 6 Power Loss Reduction for Servoless Pump Prototype Relative to Production Pump

4.4 Discussion

The experimental results align with the anticipated trends based on the servoless pump operating principles outlined in Section 2. As the swash plate angle and shaft speed increases, the increasing control valve solenoid currents indicate a larger control valve opening area is required. The overall efficiency difference is most significant at lower speeds and swash plate angles and higher pressure-differentials, conditions where the efficiency of conventional swash plate pumps is typically low.

Especially at low speeds and swash plate angles, some of the efficiency improvements of the servoless pump can be attributed to reduced cross-port flow, though the additional new dynamics of the servoless pump can also affect efficiency. For example, for the 100 bar operating conditions shown in the left panel of Figure 6, the power loss reduction is relatively constant, even as the swash plate angle and shaft speed vary. Figure 4 for the same conditions indicates that the control valve opening areas increase as both the swash plate angle and shaft speed increase. Therefore, the cross-port flow at a given speed increases as the swash plate angle increases, leading to a decrease in power loss reduction when considering cross-port flow alone. However, because the observed power loss reduction remains relatively constant, there are clearly other effects beyond just cross-port flow reduction involved that affect the power loss reduction in the servoless pump.

Upon initial inspection of the 100 bar results of Figure 6, it seems as if the efficiency improvement of the servoless pump should be constant across swash plate angles, not trending downwards as shown with the 100 bar results of Figure 5. This behavior can be explained by substituting Equation (5) into Equation (2), reformulating the overall efficiency to be a function of the input power and power loss:

$$\eta_\tau = \frac{P_{in} - P_{loss}}{P_{in}} = 1 - \frac{P_{loss}}{P_{in}} \tag{6}$$

The overall efficiency difference, $\Delta\eta_\tau$, between two pumps with the same rotating kit that are running at the same operating conditions (swash plate angle, shaft speed, pressure differential, and temperature) can be rewritten as:

$$\Delta\eta_\tau = 1 - \frac{P_{loss,2}}{P_{in}} - \left(1 - \frac{P_{loss,1}}{P_{in}}\right) = \frac{P_{loss,1} - P_{loss,2}}{P_{in}} = \frac{\Delta P_{loss}}{P_{in}} \tag{7}$$

where ΔP_{loss} is the power loss reduction of the second pump relative to the first pump. When the rotating kit is unchanged between the pumps and the primary efficiency improvements are due to hydraulic efficiency improvements (as is the case for the servoless pump prototype), the input power should not change significantly between the pumps. As the swash plate angle increases, so does the shaft torque, leading to an increased input power. Inspection of

Equation (7) shows that a constant power loss reduction leads to a reduced efficiency improvement as the input power increases.

The servoless pump prototype used in the tests is a proof-of-concept intended to show displacement controllability of a servoless swash plate pump and was designed with the sole intent of demonstrating that the pump displacement could be controlled using only forces generated by the rotating kit. It is likely that the efficiency of the pump can be improved beyond the results shown here, especially at the higher swash plate angles.

5 Comparison of Simulation Model to Experimental Results

A simulation model was constructed in Simulink, mirroring the assumptions and functionality outlined in Section 3. The simulations were conducted at the same nominal operating conditions and with the same oil properties as those used in the experimental tests. Both the production pump and servoless pump were simulated. Nominal dimensions and values were used for both pumps.

5.1 Overall Efficiency Difference Comparison

Figure 7 demonstrates the simulation predictions of overall efficiency difference between the servoless pump and production pump to the experimental results. The simulation results follow the same trends as the experimental results and are generally within measurement accuracy of the experimental data at swash plate angles 12° and above. Apart from the 1,000 RPM, 200 bar operating conditions, the simulation tends to underpredict the overall efficiency difference.

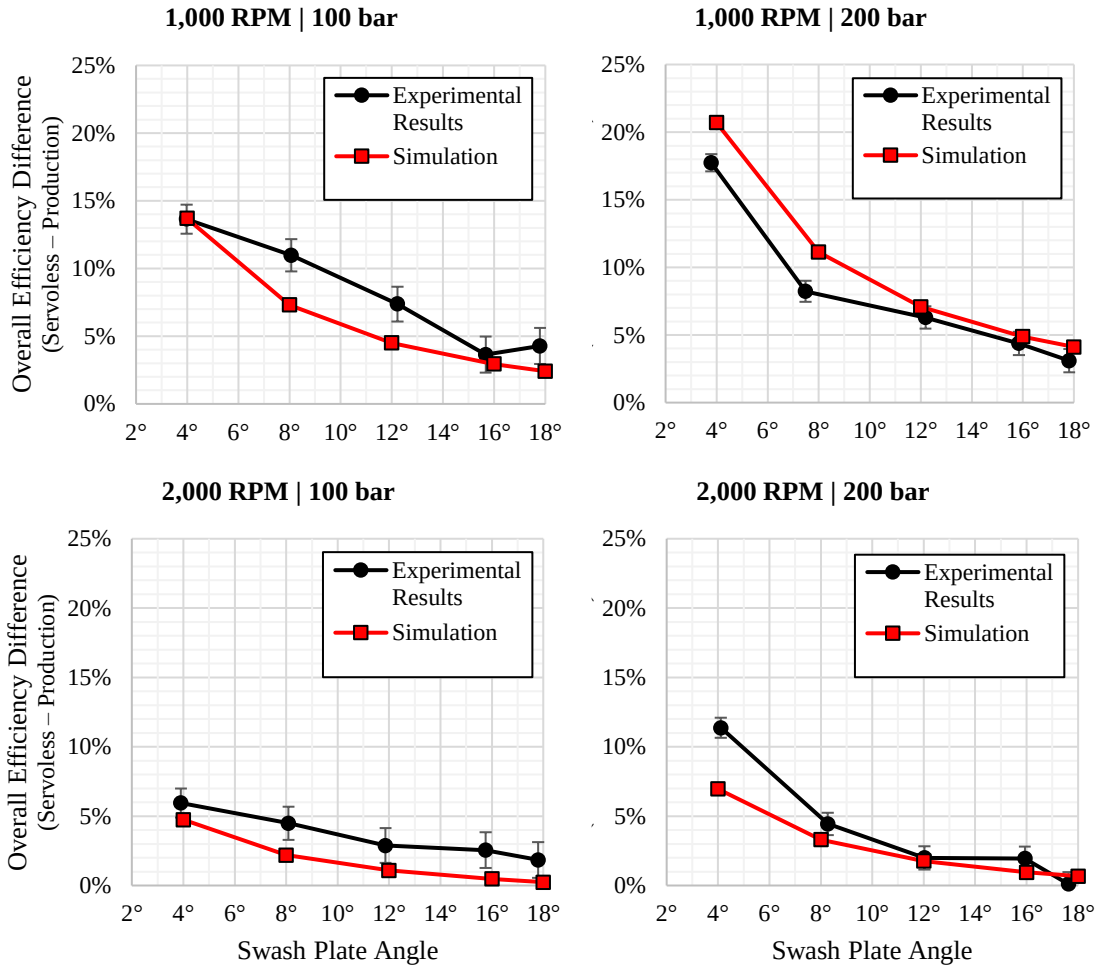

Figure 7 Overall Efficiency Difference, Simulation vs. Experimental Results

5.2 Discussion

The correlation between the simulation results and experimental results is impressive considering the modeling approach and early stage of investigation of the servoless pump concept. Although 1D modeling is a powerful tool, there are many aspects of a pump it cannot fully capture that have an impact on performance (for example, deformations and fluid film thicknesses/gap heights). That said, such close agreement validates the servoless pump theory and enhances confidence in the predictive capabilities of the simulation model. Even with the discrepancies between the model predictions and the experimental results, the accuracy is sufficient for design and optimization purposes because of good qualitative and quantitative agreement, especially at high swash plate angles. The servoless pump is a new concept, and the accuracy of the models is reasonable given the early stages of investigation.

Further work to improve the correlation between the simulation and experimental results is planned. The operating conditions in this comparison are only a subset of the operating conditions of a typical pump. Higher pressures and speeds and motoring operating conditions are also important. Additionally, improved correlation with the current model would likely be recognized by using measurements of the tested hardware rather than nominal values. Tuning friction and loss coefficients to the tested hardware can also be done. With these improvements in mind, there is significant potential for improved correlation between the simulation and experimental results, especially at low swash plate angles.

6 CONCLUSION

The servoless swash plate unit is an innovative technology that replaces a traditional servo piston for stroke control with a dynamic valve plate that controls swash plate moments. Controllability of a servoless swash plate pump was demonstrated in previous work, but that work did not investigate the potential efficiency improvements. The servoless/dynamic swash plate approach theoretically provides improved efficiency due to elimination of servo system losses and reduction of cross-port flow, and that theory was validated in this work. A production 130 cc swash plate pump was tested, modified to function as a servoless pump, and retested. The servoless pump showed improved efficiency over the production pump at all tested conditions, peaking at an overall pump efficiency improvement of nearly 18%. Similarly, the servoless pump shows a power loss reduction between 1 and 2 kW when compared with the production pump. The efficiency improvements and power loss reductions presented in this paper apply only to the rotating kit of the pump – they do not account for the power loss of the production pump servo system or the electrical power needed to drive the control valves. Note that the servoless pump used in this experimentation was a proof-of-concept design intended to demonstrate controllability. It has not been optimized for efficiency, and further improvements are likely.

Simulating a servoless swash plate unit and a conventional swash plate unit are largely the same, but shortcuts sometimes used in conventional pump modeling cannot always be taken. Moments applied to the swash plate by the rotating kit are now the control force instead of disturbances, and care must be taken to account for effects such as piston inertia, friction, and leakage. Furthermore, the swash plate must dynamically respond to the moments applied to it within the model. Such a model was implemented in Simulink and the simulations were conducted to mirror the experimental operating conditions. The simulation predictions for overall efficiency difference between the servoless and production pumps follow the same trends as the experimental results and are generally within ±3% of the experimental results and often within ±2%. This correlation is impressive for a 1D simulation model that lacks subtleties such as deflection and non-uniform gap heights, and the simulation results are well within the range of being useful for design and optimization work.

The advancements showcased in this work underscore the promising potential of servoless swash plate pumps, offering not only significant efficiency improvements but also aligning well with industry megatrends of sustainability and emissions reduction. With minimal modifications to existing production pump hardware, the adoption of this technology presents a compelling pathway towards improved efficiency and reduced environmental impact, marking a significant stride forward in fluid power systems innovation.

7 REFERENCES

[1] R. W. Reynolds, "ROTARY PUMP WITH DISPLACEMENT CONTROL". United States Patent US3727521A, 17 April 1973.

[2] K. Miki and Y. Kotake, "VARIABLE DISPLACEMENT PISTON MACHINE". United States Patent US4918918A, 24 April 1990.

[3] T. A. Watts, "VARIABLE DISPLACEMENT AXIAL PISTON HYDRAULIC UNIT". United States Patent US005554007A, 10 September 1996.

[4] C. Junhee, "Dynamic Modeling and Analysis for Swash-Plate Type Axial Pump Control Utilizing Indexing Valve Plate," ProQuest, 2000.

[5] J. Tvarůžek, R. Rahmfeld, C. Fiebing, A. Krahn and W. Göllner, "DYNAMIC VALVE PLATE DESIGN FOR AN AXIAL PISTON PUMP (SERVO-LESS PUMP)," in *14th IFK Proceedings*, Dresden, 2024.

[6] R. Rahmfeld, "Displacement Machines – Key Elements of Future Technology (General Lecture)," in *12th International Fluid Power Conference (12. IFK)*, Dresden, 2020.

[7] "Hydraulic fluid power – Positive-displacement pumps, motors, and integral transmissions – Methods of testing and presenting basic steady state performance," ISO 4409:2019(E), 2019.